

Amorphous Materials: Ionic Transport

Since the experiments of Warburg in the 1880s, it has been known that glass behaves as a solid electrolyte when the temperature is high enough (typically over 300°C for a common soda-lime-silica glass), and that the current carriers are predominantly monovalent cations (Angell 1990, Hughes and Isard 1972, Ingram 1987). Work on ionically conducting glasses is now driven by the demand for electrochemical sensors, all-solid-state batteries, and by the need to develop a satisfactory theory of the observed phenomena which include frequency-dependent conductivities, mixed cation effects, and superionic conductivity. Detailed treatments of these topics are given in the relevant articles. This article deals mainly with the search for a satisfactory understanding of ion transport in amorphous materials.

1. Experimental Conductivity Measurements

Nowadays almost all ionic conductivities are obtained from a.c. measurements. This minimizes the intrusion of electrode polarization (mainly seen at lower frequencies) and of dielectric dispersion phenomena (observed at higher frequencies). A.c. data collected on automated frequency-response analyzers are presented graphically in several ways (Ingram 1987). Figure 1 illustrates one of the more widely used procedures and shows part of the conductivity spectrum for a commercial soda-lime-silica glass measured over a range of temperatures. Contact to the sample is made by painting on silver electrodes. The “d.c.” conductivity is actually the plateau value measured over a range of frequencies.

2. Variations in Conductivity with Temperature and Pressure

Figure 2 (Ingram 1987) shows how conductivities vary with temperature for two glasses, shown as an Arrhenius plot of $\log_{10}\sigma$ as a function of reciprocal temperature. Consider first the lower curve, which is for the sodium trisilicate ($\text{Na}_2\text{O}:3\text{SiO}_2$) system. The curved line represents the behavior of the molten silicate; below the glass transition temperature (T_g) the graph is linear. This is typical behavior (Souquet and Jayasinghe 1996). Above T_g , conductivities normally follow the Vogel–Tamman–Fulcher (VTF) equation:

$$\log_{10}\sigma(\text{or } \sigma T^{1/2}) = \log_{10}\sigma_0 - \frac{B}{T - T_0} \quad (1)$$

where σ_0 is a pre-exponential factor, B (in K) is an empirical fitting constant, and T_0 is a “zero-mobility

temperature” normally less than T_g . Below the experimental T_g , conductivities follow the Arrhenius equation:

$$\log_{10}\sigma(\text{or } \log\sigma T) = \log_{10}\sigma_0 - \frac{E_a}{2.303RT} \quad (2)$$

where E_a is an experimentally defined energy of activation.

As a rule, high conductivities in glass are associated with low activation energies and vice versa. Silver iodoborate ($\text{Ag}_3\text{I}_4\text{BO}_2$) is a typical “superionic” glass. These glasses (Fig. 2) have ambient-temperature conductivities in the region of 10^{-2} Scm^{-1} , and are discussed in a separate article (see *Glasses: Superionic*).

Ionic conductivities are also measurable as a function of externally applied (hydrostatic) pressure (Fanggao *et al.* 1996). Such experiments allow calculation of activation volumes ΔV^* :

$$\frac{d\ln\sigma}{dP} = \frac{-\Delta V^*}{RT} \quad (3)$$

where the volume of activation may be thought of as an “excess” volume which becomes available to an ion when it moves. Generally, ΔV^* increases with increasing ion size ($\text{Li}^+ < \text{Na}^+ < \text{Ag}^+ < \text{K}^+$) and can vary if a given cation (e.g., Ag^+) is hosted by different glass matrices. In this latter case ΔV^* always decreases as E_a decreases.

3. The Concept of Decoupling

The idea that ion transport processes are decoupled from structural relaxations occurring in highly viscous molten salts is well established (Moynihan *et al.* 1971). Two kinds of relaxation process are distinguished. First, there is the viscous flow relaxation time, which is given by $\tau_{\text{mech}} = \tau_s = \eta/G$, where η (in Pa s) is the shear viscosity and G (in Pa) is the shear modulus. This relaxation process is a property of all the atomic or molecular entities in the liquid. Second, there is a corresponding electrical or “conductivity” relaxation time, given by $\tau_{\text{elec}} = RC = \varepsilon_r\varepsilon_0/\sigma$, where ε_r is the relative permittivity of the melt, ε_0 is the permittivity of free space, and σ (in Scm^{-1}) is the d.c. conductivity. This relaxation time is again a macroscopic property of the system, but many authors find it useful to consider $\tau_{\text{elec}} = \tau_\sigma$ in a more atomistic way as an “average residence time” for ions located on sites in the melt.

If the ratio $\tau_{\text{mech}}/\tau_{\text{elec}}$ is close to unity, ionic motions and the structural relaxations giving rise to viscous flow are strongly coupled. However, if the ratio τ_s/τ_σ is

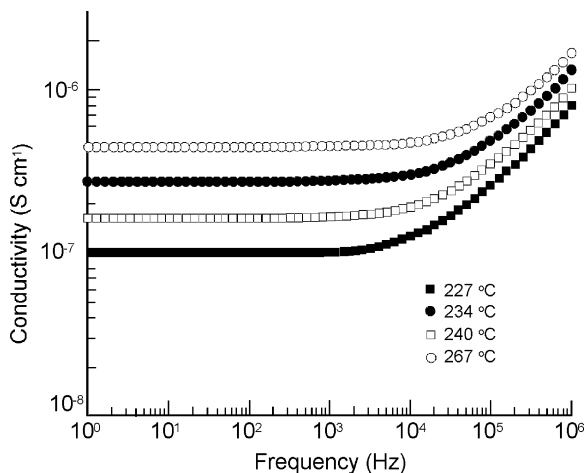


Figure 1
Conductivity data for a commercial soda-lime–silica glass (glass slide) plotted as a function of frequency at different temperatures. The d.c. conductivities are the plateau values (data from M. H. Wu, Aberdeen, UK).

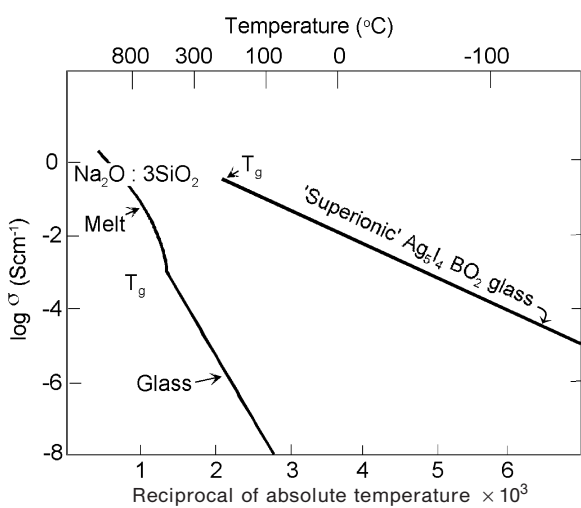


Figure 2
Arrhenius plots of conductivity for molten and glassy sodium trisilicate and for “superionic” $\text{Ag}_5\text{I}_4\text{BO}_2$ glass (after Ingram 1987).

much greater than one, ionic movements occur without involving viscous flow (or relaxation of mechanical stresses), and ionic motions and structural relaxations are said to be decoupled from each other. Generally, the degree of decoupling increases as the melt is cooled towards T_g , where the structural relaxation can be identified by the change in heat capacity, normally

detected by DSC, or in the mechanical modulus detected by mechanical spectroscopy.

On the basis of these ideas, Angell (1986, 1990) defined a decoupling index R_τ , such that:

$$R_\tau(\text{mech}) = \frac{\tau_s}{\tau_\sigma} \quad (4)$$

or

$$R_\tau(\text{thermal}) = \frac{\tau_H}{\tau_\sigma} \quad (5)$$

where τ_σ is obtained from $\varepsilon_r \varepsilon_0 / \sigma$, measured at the glass transition temperature, T_g , and τ_s or τ_H are shear or enthalpy relaxation times measured appropriately.

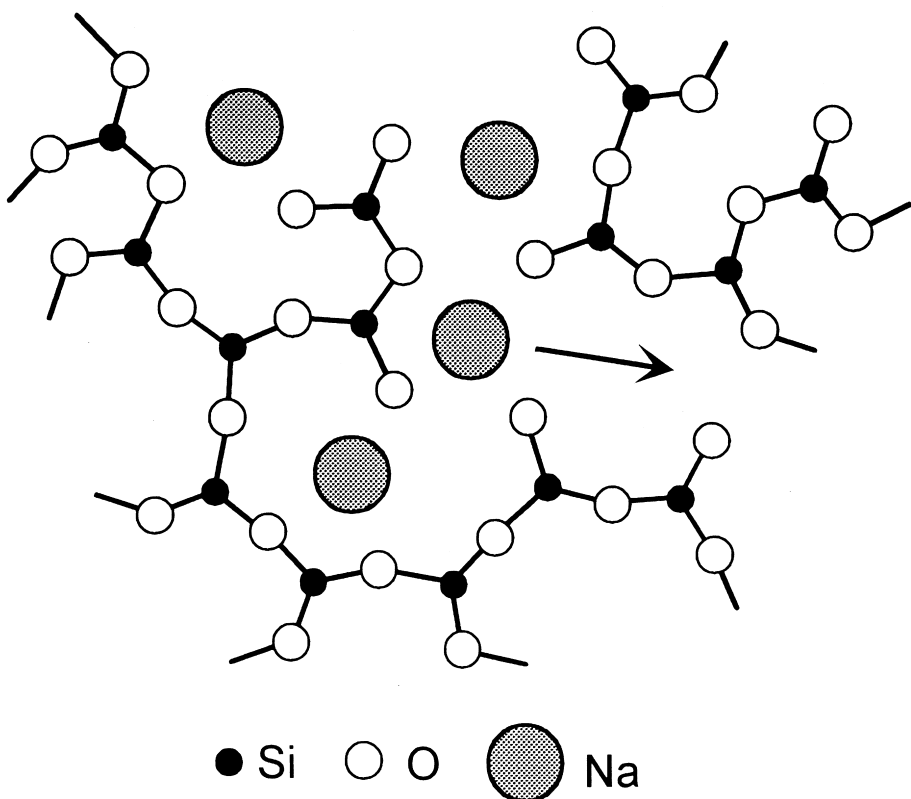
The glass transition temperature is a conveniently defined kinetic reference point. Thus as a liquid is cooled through T_g , it solidifies because structural relaxations (involving molecular and atomic displacements) occur too slowly to influence the mechanical and thermal properties. The time scale for observing these relaxations is defined by the experiment. In a torsional pendulum experiment, $\tau_{\text{mech}} = 1/\omega = 1/2\pi f$ where f is the frequency of oscillation. In a typical DSC experiment where the heating rate is 10 K min^{-1} , $\tau_H \approx 100 \text{ s}$. Values of R_τ can be very high: typically around 10^{12} for the sodium trisilicate glass and 10^{14} for the silver iodoborate glass illustrated in Fig. 2.

A simple picture of how decoupling comes about is shown in Fig. 3, which is based on Warren and Biscoe's (1938) representation of Zachariasen's random network model for silicate glasses. The silicon atoms are drawn as three-coordinated (not four) to make it easier to distinguish bridging from non-bridging oxygens (BOs and nBOs) and to identify the sites (or interstitial spaces) which are available to the mobile Na^+ ions. Note that Na_2O acts as “network modifier” and as a source of both nBOs (which are negatively charged) and the mobile Na^+ ions. The large values of R_τ found in these glasses point to an essentially solid-like conduction mechanism in glass.

4. Ways of Increasing Glass Conductivity

4.1 Simple Network Glasses

Almost universally, the electrical conductivity of network glasses increases with increasing alkali oxide (or modifier) content. The effect is pronounced in $\text{Na}_2\text{O}-\text{B}_2\text{O}_3$ glasses (Fig. 4) (Ingram 1987). The conductivity at 300°C increases by five orders of magnitude as the Na_2O content is increased from 10% to 30%. Further additions of Na_2O (and/or Na_2SO_4 as “dopant”) bring about a corresponding (100-fold) increase in conductivity before the limit of glass formation is reached.

**Figure 3**

The solid-like conductivity mechanism in typical “silicate” glass, where silicon is drawn three-coordinate for clarity (based on Warren and Biscoe’s early ideas).

4.2 The Action of Dopant Salts

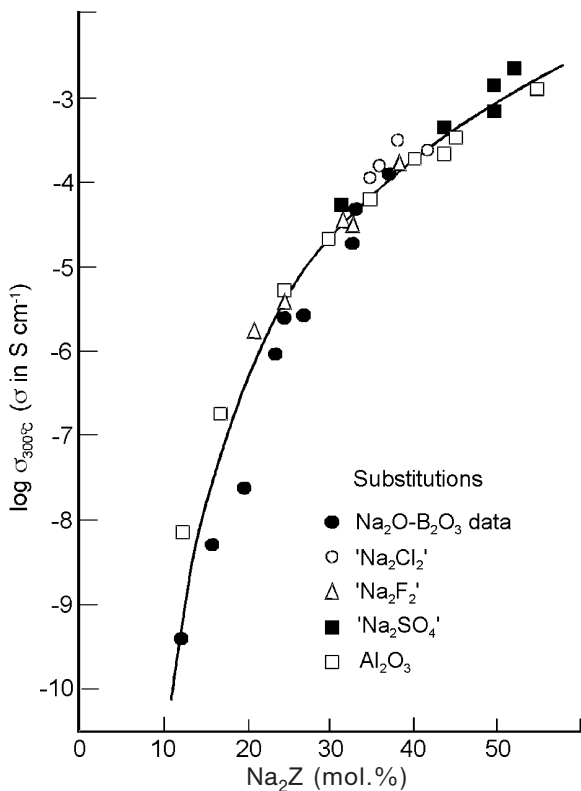
Figure 4 contains data for glasses in an enlarged $\text{Na}_2\text{O}-\text{B}_2\text{O}_3$ system, where the range of glass formation has been increased either by replacing B_2O_3 by Al_2O_3 or by introducing dopants such as “ Na_2Cl_2 ,” “ Na_2F_2 ,” and Na_2SO_4 in place of Na_2O . Effectively, glass formation is being extended by use of the “confusion principle” which acts to suppress crystallization. Use of dopant salts such as LiCl and Li_2SO_4 to enhance the conductivities of lithium borate and lithium phosphate glasses and of mixed oxysulfide glasses is a guiding principle widely used in the design and selection of glass compositions for lithium battery applications (see *Batteries: Glassy Electrolytes* for more details).

4.3 Optimized Ionically Conducting Glasses

A detailed discussion of ways of optimizing ionic conductivity in glass belongs to the topic of superionic glasses (see *Glasses: Superionic*). Two examples of

superionic glass behavior, however, fit conveniently into this general discussion. First, there is the use of Al_2O_3 as “network reinforcer” in alkali aluminosilicate glasses. The effect of adding Al_2O_3 is to replace nBOs with negatively charged aluminosilicate groups ($\text{Al}\emptyset_4^-$) where \emptyset denotes oxygen atoms shared by aluminum and silicon atoms. These glasses show very high values of T_g (over 700°C at large Al_2O_3 contents) and enhanced alkali cation mobilities. They are also good ion exchangers which are used in chemically strengthened glass and in the production of graded (refractive) index glasses (see *Amorphous Materials: Mixed Alkali Effect*).

Second, there are the glasses with high ambient conductivities (Fig. 2) produced by combining AgI with a range of Ag_2S - or Ag_2O -based materials, which contain either networks (e.g., borates) or discrete anions (e.g., molybdates), which may or may not form glasses by themselves. The conductivity of these glasses always increases with increasing AgI content. Such increases are now associated with structural changes and with associated increases in free volume (Swenson and Börjesson 1998).

**Figure 4**

Conductivities at 300°C in the “enlarged” sodium borate system as a function of total sodium oxide plus dopant salt concentration (after Ingram 1987).

5. Mechanisms of Ion Transport

5.1 The “Classical Model”

According to Anderson and Stuart (1954), the energy barrier for site-to-site hopping in glass is given by:

$$E_a = E_b + E_s \quad (6)$$

where E_b is an electrostatic energy binding the ion to its site and E_s is an elastic strain energy required to open up doorways to allow ions to pass from site to site. A common expression for E_b (e.g., Rao *et al.* 1993) is:

$$E_b = \frac{zz_0e^2}{\gamma(r+r_0)} - \frac{zz_0e^2}{\gamma\lambda/2} \quad (7)$$

where ze and z_0e are charges on the cation and nBO respectively, r and r_0 are corresponding ionic radii, λ is the intersite distance, and γ is a “covalency parameter”—sometimes identified arbitrarily with the relative permittivity, ϵ_r , of the glass. It is assumed tacitly in the classical model that all sites lie on

percolation pathways extending throughout the glass, and that all empty sites are equivalent to each other.

This model still attracts attention because of its inherent simplicity. A highly schematic view of what is implied was given by Martin and Angell (1986) (Fig. 5). The sites are shown far enough apart for the escape of the ion and its subsequent passage through the doorway to occur as separate steps. The model has enjoyed two main successes.

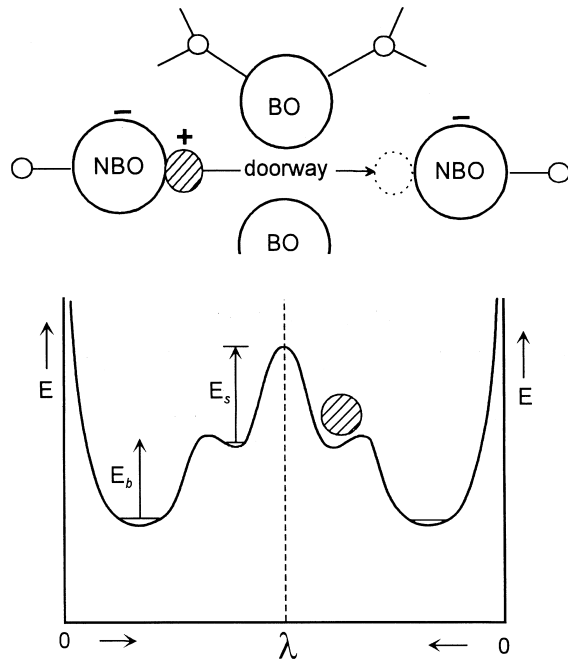
First, it made sense of the lower activation energies for ion transport found in alkali aluminosilicate glasses where the spreading out of negative charge from nBOs to AlO_4 tetrahedrons, where \emptyset represents and oxygen bridging Al to Si, leads to an effective increase in “ r_0 ” and a decrease in electrostatic binding energy, E_b . Second, it assisted in the selection of superionic glass compositions during the rapid expansion in the field of solid-state ionics in the 1970s and 1980s. According to the model of Anderson and Stuart (1954), conductivity in glass is enhanced by an increase in covalency which implies the need for a “softer” glass matrix containing larger, more polarizable anions. This reasoning pointed initially to the inclusion of chlorides, bromides, and iodides as dopant salts and to the replacement (or partial replacement) of oxide ions in the network by sulfide and selenide as ways of facilitating cation transport.

Nevertheless, the simple classical picture is inadequate. First, the model is not microscopic, since it takes no account of details of the coordination polyhedrons actually occupied by the cations. Second, since it makes no allowance for a spatial distribution of sites, it cannot deal either with percolation effects or with the long-range Coulomb forces.

The first question has been addressed by several authors (Rao *et al.* 1993, Elliott 1994) who considered transport to involve ions “rolling” between adjacent coordination polyhedrons. These authors considered that the concept of isolated Coulomb traps would be valid only at low cation concentrations: at higher concentrations, the energy barrier is determined mainly by changes in polarization energy and by short-range cation–anion interactions.

The second question, relating specifically to percolation and long-range Coulomb effects, has been addressed by Monte Carlo (MC) simulations of simple lattice-gas models (Knödler *et al.* 1996). They investigated the diffusive dynamics of particles of charge q in an energy landscape determined by immobile centers of charge ($-q$) distributed randomly in space (these correspond to the nBOs in Fig. 3).

The advantage of such simulations is that an idealized model can be precisely defined and its consequences then evaluated. Details of actual glass structure are not included in the modeling. Nevertheless, Knödler *et al.* (1996) included some essential ingredients of static disorder (involving the Coulomb traps generated by the fixed charges) and of dynamic disorder (involving Coulomb repulsions between mo-

**Figure 5**

A pictorial representation of the classical ion-hopping model incorporating ideas based on the weak electrolyte theory (λ is the intersite separation). The lower figure shows a “free” ion located in a higher energy (interstitial) site (after Martin and Angell 1986).

bile ions). The simulations focused on the dilute cation region, where this approach is likely to be valid (see the comments of Rao *et al.* (1993) and Elliott (1994)) and successfully delivered a power-law relationship between conductivity and cation content:

$$\sigma = \text{const.} \times c^p \quad (8)$$

where $p \approx 1/T$ (see below). In a very general way, the success of the MC simulations supports the validity of the classical approach, even though such matrix-specific factors as elastic strain energy are not included.

5.2 Alternatives to the Classical Model

(a) *The weak electrolyte theory.* Ravaine and Souquet (1977) examined the phenomenon of ion transport in glass from the more general standpoint of electrolyte theory where ionic conductivity is expressed as the product of concentration and mobility terms:

$$\sigma = n^* z e v \quad (9)$$

where z is the charge number and e the electronic charge (as before), n^* is the number of “mobile” ions

per unit volume, and v is the corresponding electrical mobility (in units of $\text{cm s}^{-1} \text{V}^{-1} \text{cm}^{-1}$).

Aqueous electrolytes (such as acetic acid, CH_3COOH) are weak electrolytes in the sense that the conductivity is determined by concentrations of free ions (in this case of CH_3COO^- and H_3O^+) which are *equilibrium* properties of the system. Ravaine and Souquet (1977) (R-S) suggested that similar dynamic equilibria exist in glass, and that it is possible to distinguish mobile from immobile cations. In pictorial terms, cations in the deeper sites (Fig. 5) may be considered as being trapped or immobile, while ions in the shallower sites are free or mobile. If a given fraction of ions exist outside the deep sites, then E_b of the classical model may be thought of as an energy of dissociation, and E_s is the energy of migration.

R-S described the escape of cations from their traps in sodium silicate glasses by a chemical equilibrium:



where SiO_2 is left out of the equation for simplicity. From conventional thermodynamics, the chemical potential of Na_2O is given by:

$$\mu_{\text{Na}_2\text{O}} = \mu_{\text{Na}_2\text{O}}^0 + RT \ln a_{\text{Na}_2\text{O}} \quad (11)$$

$$= \mu_{\text{Na}_2\text{O}}^0 + RT \ln [\text{Na}^+] [\text{ONa}^-] \quad (12)$$

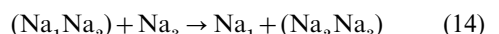
which assumes that activity coefficients are constant (so ionic activities = ionic concentrations) since, according to the model, the concentrations of “free” Na^+ ions are small, and which ignores the (possibly profound) influence of the “undissociated” Na_2O on the overall glass structure (and hence on the way $\mu_{\text{Na}_2\text{O}}^0$ might vary with Na_2O concentration).

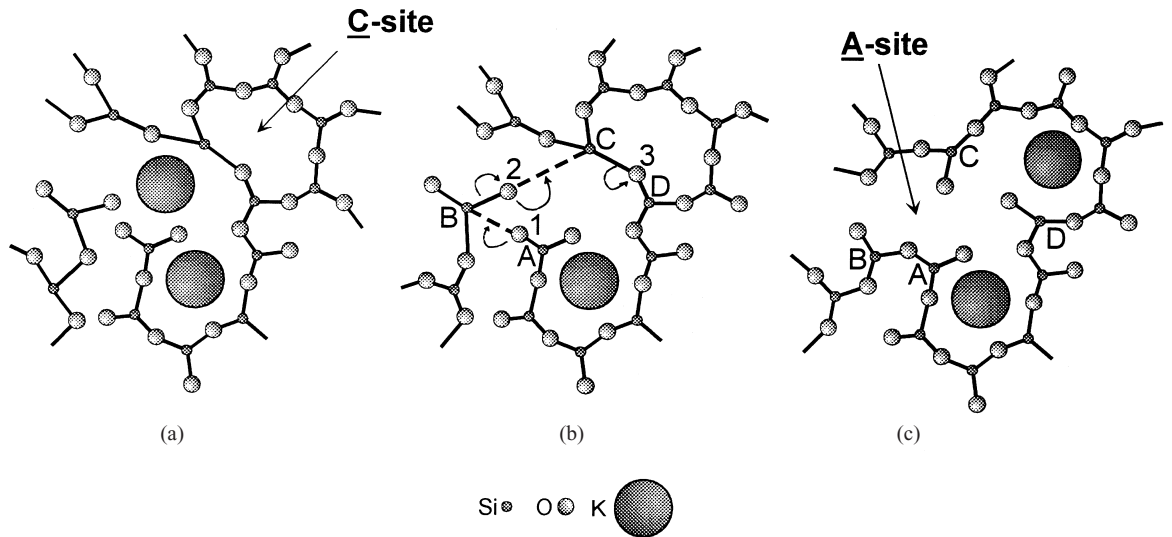
Comparing Eqns. (11) and (12), it is apparent that $[\text{Na}^+] = (a_{\text{Na}_2\text{O}})^{0.5}$, and so if the mobility of free Na^+ ions remains constant:

$$\sigma \propto (a_{\text{Na}_2\text{O}})^{0.5} \quad (13)$$

Experimental support for Eqn. (13) from data for $\text{Na}_2\text{O}-\text{SiO}_2$ glasses seems to justify the assumptions made in this theory. Interest in the field of glassy ionics in the late 1970s was greatly stimulated by the publication of the R-S paper.

One way of extending the R-S model is to identify the mobile ions with the presence of “defects” in the glass, such as cation pairs (Ingram 1987). This involves the concept of “double sites” which can be either singly or doubly occupied. The arrival of a second cation at a singly occupied double site will “trigger” the departure of a cation which is already there. Such a process is an exchange of partners reaction, and this “interstitialcy” process can be written as:



**Figure 6**

A schematic view of the dynamic structure of molten potassium silicate glass where cooperative bond rearrangements in the silicon–oxygen network are triggered by the movement of an ion. Note how a C site in (a) is “upgraded” to an A site in (c), and how an empty A site is created which can act as a stepping stone for subsequent ion hopping after the melt is frozen to a glass. In (b) one of the $\text{K}^+(\text{A}^+)$ ions is removed, to allow the movement of electron pairs (curly arrows) to be observed.

where the species in parentheses are interstitial pairs. Note that Na_1 is (temporarily) immobilized as a result of this process, while Na_3 is now free to move. This model has been further developed (Elliott and Owens 1989) as a “diffusion-controlled relaxation model”, and in this form successfully accounts for some of the a.c. properties of glass including conductivity dispersions observed at higher frequencies.

Nevertheless, the weak electrolyte theory is still debatable. In contrast to the situation that exists in aqueous electrolytes, it is very difficult in glass to specify the concentration of mobile ions (i.e., to specify equilibrium constants for processes such as Eqn. (10)). Different methods of evaluating n^* tend to give different answers (e.g., Agrawal *et al.* 1996, Roling *et al.* 1997), and some approaches which look promising may actually be inapplicable.

A good example of such a debatable approach is that based on the Nernst–Einstein equation. In its simplest form, this can be written as:

$$\nu_i = \frac{D_i e}{k_B T} \quad (15)$$

where ν_i and D_i are electrical mobilities and diffusivities, respectively, for mobile monovalent cations. An obvious step would be to calculate values of ν_i from D_i and to obtain corresponding values of n^* by substituting into Eqn. (9). However, according to the weak electrolyte models for glass which have been

discussed so far (either in Eqns. (10) or (14)), it is the same free ions which contribute to conduction and diffusion. In other words, if a Na^+ ion is free to diffuse in a sodium silicate glass it also conducts. This is very different from the situation which occurs in a molten salt where ion pairs may be present, which in principle can diffuse but are not influenced by an electric field. It is more difficult to envisage such “currentless diffusion” in a glass.

Nevertheless, the Nernst–Einstein equation does supply useful evidence in support of a defect-based solid-state mechanism. Combining Eqns. (9) and (15), and setting $n = n^*$, gives:

$$D(\sigma) = \frac{\sigma k_B T}{ne^2} \quad (16)$$

$D(\sigma)$ is not necessarily equal to D_i obtained by tracer methods. In fact $D_i/D(\sigma)$ is termed the Haven ratio (H_R) and is commonly less than unity ($H_R \approx 0.5$). Such a value would be expected, for example, for a collinear interstitialcy process (as in Eqn. (14)), where the two cationic charges are carried forwards for each step of the diffusing ion.

(b) *The dynamic structure model (DSM).* The central idea of the DSM (Bunde *et al.* 1994) is that sites are created in response to the needs of the cations.

Thus, in single and in mixed Na^+/K^+ ion glass, Na sites are created for Na^+ ions, and K sites for K^+ . Structure building in the molten or solid glass depends on the dynamic responses of the network to the moving ions.

To test this idea, Bunde *et al.* (1994) performed MC simulations. The mobile ions were placed (for convenience) on square or cubic lattices and the dynamic response of the network was simulated by a site-switching mechanism which converted “unimproved” cation sites (C) into A sites, optimized in terms of size, coordination number, and appropriate mix of BOs and nBOs to the needs of the outgoing A^+ ions. These A sites then became the “stepping stones” (preferred targets) which defined percolation pathways for transport of A^+ ions through the glass. In cation-rich glasses, A sites are plentiful and the conductivity is high. In cation-poor glasses, A sites are in short supply and ion migration is more difficult. In these latter glasses, it becomes necessary for A^+ ions to jump mainly into C sites, where hopping rate is given by:

$$\bar{\omega}_{AC} = \bar{\omega}_{AA} \exp \left(\frac{-T_1}{T} \right) \quad (17)$$

where $T_1 = E_a^*/k_B$, k_B is Boltzmann's constant, and E_a^* is an additional activation energy (a mismatch relaxation energy) required to make the C site habitable to the incoming A^+ cation. It was further postulated that an additional relaxation time, τ , would be needed for the (occupied) C site to be fully converted into an A site.

The notable success of the DSM was that it led to the discovery of the power-law dependence of conductivity on concentration, $\sigma = \text{const.} \times c^\rho$, where $\rho \propto 1/T$, which was recognized first in these computer simulations, then in experimental data, and finally was confirmed by the computer simulations of Knödler *et al.* (1996), based on the fixed counterion model (see Eqn. (8)). The extension of the DSM to include effects seen in mixed-cation glasses is discussed in *Amorphous Materials: Mixed Alkali Effect*.

(c) *Static or dynamic structures for glassy materials?* It is remarkable how two quite different percolation models, one based on an energy landscape determined by Coulomb interactions and fixed counterions (nBOs) and the other on a landscape determined by earlier movements of the mobile ions, can give rise to the same (correct) power-law dependence of conductivity on composition. The question is: does it make more sense to consider glass structure in terms of the static or dynamic models?

Figure 6 shows a breakdown of the processes involved in moving a cation into a nearby C site (where there are no surrounding nBOs), including the transfers of some nBOs from silicon atoms A and B to

C and D, and a distribution of nBOs resulting in the creation of a new A site while leaving an A site behind for another ion to jump into. Clearly, atoms A–D all experience a change in “Q” (the number of BOs per silicon) as a result of this site conversion process. However, the NMR measurements of Stebbins and Sen (1997) show that such silicate isomerization processes normally occur at measurable speed in molten silicates, and so the conclusion could be that such A/C relaxations can normally occur only in the melt. In that sense, there is no irreconcilable difference between a dynamically *determined* structure model (where A and C sites are created in the melt and persist in the glass) and the classical viewpoint, with a static structure, as embodied in the simulations of Knödler *et al.* (1996). However, it is possible that cation movements can induce milder forms of network relaxation even far below T_g (which would put a new gloss on Angell's decoupling concept).

6. The Way Forward

There is now a wealth of information concerning ion transport in glass and no shortage of ideas relating to underlying chemical and physical principles. Future developments in glassy ionics are likely to focus on practical applications in electrochemistry, e.g., in connection with the still widespread use of ion-selective glass electrodes in chemical analysis (Bauke 1996), and with dealing in more detail with microscopic aspects of ion transport making use of relevant structural information (Greaves and Ngai 1995) and, if necessary, of molecular dynamics simulations. If these theoretical approaches are to contribute significantly to practical applications, then there will need to be more recognition of the importance of interfacial phenomena and of what happens when ions (and also electrons) are introduced into or withdrawn from the amorphous matrix. Almost certainly this practical emphasis will focus more attention on the dynamic aspects of the ion–matrix interaction which until now have been somewhat neglected.

See also: Glasses: Superionic; Conducting Materials: Solid-ionic and Super-ionic

Bibliography

- Anderson O L, Stuart D A 1954 Calculation of activation energy of ionic conductivity in silica glasses by classical methods. *J. Am. Ceram. Soc.* **37**, 573–80
- Angell C A 1986 Recent developments in fast ion transport in glassy and amorphous materials. *Solid State Ionics* **18–19**, 72–88
- Angell C A 1990 Dynamic processes in ionic glasses. *Chem. Rev.* **90**, 523–42
- Agrawal R C, Kumar R, Chandra A 1996 Transport studies on a new fast silver ion conducting system: 0.7 [0.75AgI: 0.25AgI]. 0.3 [$y\text{Ag}_2\text{O}:(1-y)\text{B}_2\text{O}_3$]. *Solid State Ionics* **84**, 51–60

- Baucke F G K 1996 Glass electrodes: why and how they function. *Ber Bunsenes. Phys. Chem.* **100**, 1466–74
- Bunde A, Ingram M D, Maass P 1994 The dynamic structure model for ion transport in glasses. *J. Non-Cryst. Solids* **172**, 1222–36
- Elliott S R 1994 Calculation of the d.c. conductivity activation energy of ionically conducting glasses. *J. Non-Cryst. Solids* **172–174**, 1343–52
- Elliott S R, Owens A P 1989 Diffusion-controlled relaxation model for ionic transport in glasses. *Philos. Mag. B* **60**, 777–92
- Fanggao C, Saunders G A, Wei Z, Cutroni M, Mondania A, Piccob A 1996 Hydrostatic pressure effects on a.c. conductivity of the AgPO_3 and $(\text{Ag}_2\text{S})_{0.3}(\text{AgPO}_3)_{0.7}$ superionic glasses. *Solid State Ionics* **86–88**, 425–30
- Greaves G N, Ngai K L 1995 Reconciling ionic transport properties with atomic structure in oxide glasses. *Phys. Rev. B* **52**, 6358–80
- Hughes K, Isard J O 1972 Ionic transport in glasses In: Hladik J (ed.) *Physics of Electrolytes*. Academic Press, London, pp. 351–400
- Ingram M D 1987 Ionic conductivity in glass. *Phys. Chem. Glasses* **28**, 215–34
- Knödler D, Pendzig P, Dieterich W 1996 Ion dynamics in structurally disordered materials: effects of random Coulomb traps. *Solid State Ionics* **86–88**, 29–39
- Martin S W, Angell C A 1986 D.c. and a.c. conductivity in wide composition range $\text{Li}_2\text{O}-\text{P}_2\text{O}_5$ glasses. *J. Non-Cryst. Solids* **83**, 185–207
- Moynihan C T, Balitactac N, Boone L, Litovitz T A 1971 Comparison of shear and conductivity relaxation times for concentrated lithium chloride solutions. *J. Chem. Phys.* **55**, 3013–19
- Rao K J, Estournes C, Levasseur A, Shastry M C R, Menetrier M 1993 Activation barriers for d.c. conductivity in ionic glasses: classical calculations using the small cluster approximation. *Philos. Mag. B* **67**, 389–406
- Ravaine D, Souquet J-L 1977 A thermodynamic approach to ionic conductivity in oxide glasses: 1. Correlation of the ionic conductivity with the chemical potential of alkali oxide in oxide glasses. *Phys. Chem. Glasses* **18**, 27–35
- Roling B, Ingram M D, Lange M, Funke K 1997 Role of AgI for ionic conduction in $\text{AgI}-\text{AgPO}_3$ glasses. *Phys. Rev. B* **56**, 13619–22
- Souquet J-L, Jayasinghe G D K 1996 . In: Chowdari B V R, Dissanayake M A K L, Careem M A (eds.) *Solid State Ionics New Developments*. World Scientific, Singapore, pp. 145–69
- Stebbins J F, Sen S 1997 . In: Wright A C, Feller S A, Hannon A C (eds.) *Borate Glasses, Crystals and Melts*. Society of Glass Technology, Sheffield, UK, pp. 34–41
- Swenson J, Börjesson L 1998 Intermediate-range structure and conductivity of fast ion-conducting borate glasses. *J. Non-Cryst. Solids* **234**, 658–64
- Warren B E, Biscoe J 1938 Fourier analysis of X-ray patterns of soda-silica glass. *J. Am. Ceram. Soc.* **21**, 259–65

M. D. Ingram

Copyright © 2001 Elsevier Science Ltd.

All rights reserved. No part of this publication may be reproduced, stored in any retrieval system or transmitted in any form or by any means: electronic, electrostatic, magnetic tape, mechanical, photocopying, recording or otherwise, without permission in writing from the publishers.

Encyclopedia of Materials: Science and Technology

ISBN: 0-08-0431526

pp. 204–212